NASA Technical Memorandum 89819

Pretest Uncertainty Analysis for Chemical Rocket Engine Tests

(NASA-TM-89819) PRETEST UNCERTAINTY ANALYSIS FOR CHEMICAL ROCKET ENGINE TESTS (NASA) 16 p CSCL 14B

N87-20515

Unclas

G3/35 45314

Kenneth J. Davidian
Lewis Research Center
Cleveland, Ohio

Prepared for the
33rd International Instrumentation Symposium
sponsored by the Instrument Society of America
Las Vegas, Nevada, May 3-8, 1987

NASA

PRETEST UNCERTAINTY ANALYSIS FOR CHEMICAL ROCKET ENGINE TEST

Kenneth J. Davidian
National Aeronautics and Space Administration
Lewis Research Center
Cleveland, Ohio 44135

E-3465

SUMMARY

A parametric pretest uncertainty analysis has been performed for a chemical rocket engine test at a unique 1000:1 area ratio altitude test facility. Results from the parametric study provide the error limits required in order to maintain a maximum uncertainty of 1 percent on specific impulse. Equations used in the uncertainty analysis are presented.

INTRODUCTION

One of the new initiatives in the rocket community is the Orbital Transfer Vehicle (OTV) engine which is characterized by a high chamber pressure and a large exit area ratio. These engines use hydrogen and oxygen as the fuel and oxidizer and their specific impulse (I_{sp}) will exceed that of any engine currently in use. They are envisioned to transport payloads such as communications or observation satellites from the orbit of the space station to geosynchronous orbit. Since the entirety of their operation will be in space, these engines must be tested in facilities capable of simulating the high altitude conditions for which the engines were designed.

At the NASA Lewis Research Center Rocket Engine Test Facility (RETF), a vacuum test capsule was recently installed to simulate the environmental conditions which would be experienced by an OTV. The new test capsule is capable of handling a full scale OTV engine while maintaining the high altitude conditions. The nozzle area ratios currently under consideration for the OTV engine designs are approximately 1000:1 in order to attain the high performance required. However, no data have ever been taken for area ratios greater than 400:1. Therefore, any data taken in this facility for area ratios greater than 400:1 will be the first of its kind and will be considered to be "benchmark" data.

To obtain "benchmark" data, two requirements must be met. The first is an uncertainty goal for the important parameters being measured or calculated. The JANNAF (Joint Army Navy NASA Air Force) working group provides standardization to the rocket engine community and has suggested an uncertainty limit for the vacuum I_{sp} measurement of 0.25 percent (Ref. 1). To date, the best reported uncertainty value using a generally accepted measurement uncertainty methodology (Ref. 2) is 0.67 percent for the RL10 rocket engine (Ref. 3). The second requirement is a meaningful uncertainty value of the measured and calculated quantities. The purpose of this paper is to demonstrate how the second requirement is to be met at the RETF by describing a pretest analysis which calculates the uncertainty value for all measured and calculated parameters, based on the standardized test measurement accuracy methodology adopted by JANNAF and by numerous professional engineering associations (Refs. 4 to 7).

The pretest analysis determined the limits of error of the individual measurements which affect the specific impulse. An uncertainty on specific impulse of 1 percent was used as the criterion for setting maximum limits on the instrument errors.

APPARATUS AND PROCEDURE

Facility Description

The altitude test chamber in the RETF includes a test capsule, diffuser, spray cooler, ejectors, liquid drain lines, and the water detention tank. The exhaust gases of the rocket engine aid in altitude pumping by passing through a second throat diffuser before exhausting into the spray cooler. Approximately half of the exhaust gases are condensed to a liquid and pass down the drains to the water detention tank. Ejectors, driven by gaseous nitrogen, pump the remaining exhaust gases through two short stacks to the atmosphere.

The engine instrumentation system is displayed in Fig. 1. Propellant flow rates are measured by calibrated venturis while temperatures are measured using Cu/C thermocouples. A thermocouple type vacuum gauge is used to measure the vacuum reference pressure while the remaining pressures are measured by strain-gauge bridge type pressure transducers. Absolute and differential pressure transducers are used. The thrust stand is capable of measuring thrust levels to 13.3 kN (3000 lbf) and was designed to have a random error of less than ±0.05 percent of full scale. For more information on the facility (Ref. 8).

The TRADAR data acquisition system is used for all rocket engine tests. Instrumentation in the facility provide analog signals that are recorded and converted to a digital signal by an automatic data digitizer at a rate of 50 readings per second per parameter and sent to an IBM 370 computer. The computer averages the values in groups of five to provide data output at 1/10 sec intervals.

Data Reduction

This section describes the equations used to convert raw data (line pressures, line temperatures, differential pressures to the venturi throat, engine thrust, and ambient pressure) to performance data in order to evaluate the test firing.

Pressure at the venturi throat. - The throat pressure of the hydrogen and oxygen subsonic flow venturis flow meters was calculated by:

$$p_{th} = p_{line} - dp \tag{1}$$

Line contraction ratio. - The propellant line contraction ratio is defined by:

$$\beta = \frac{d_{th}}{d_{line}} \tag{2}$$

Thermodynamic properties upstream and at the throat of the venturi. - Using the measured values of fluid pressure and temperature upstream of the venturi throat, enthalpy, density, and entropy of the propellants were determined using the Gas Properties program (GASP)(Ref. 9). By assuming isentropic flow to the venturi throat, the throat pressure, calculated using Eq. (1), and the propellant entropy values were input to GASP to determine the fluid temperature, density, and enthalpy at the venturi throat.

Velocity at the venturi throat. - The velocity of each fluid was determined by:

$$V_{th} = \sqrt{\frac{(h_{line} - h_{th})*K}{\left[1 - \left(\frac{\rho_{th}}{\rho_{line}}\right)^2 \beta^4\right]}} \tag{3}$$

where K is a conversion constant.

Propellant mass flow rate. - The mass flow rate was determined from:

$$\dot{m} = C_d A_{th} \rho_{th} V_{th} \tag{4}$$

Total mass flow rate - The total mass flow rate is simply the sum of the mass flow rates of each fluid, namely:

$$\dot{m}_{TOT} = \dot{m}_{ox} + \dot{m}_{fu} \tag{5}$$

Vacuum thrust. - Since the site thrust was measured in an imperfect vacuum, a correction was applied:

$$F_{vac} = F_{site} + p_{amb} A_{exit} \tag{6}$$

Vacuum specific impulse. - The performance parameter of most interest to the rocket engine community is the vacuum specific impulse. This parameter is calculated by:

$$I_{sp} = \frac{F_{vac}}{\dot{m}_{TOT}} \tag{7}$$

Uncertainty Analysis Methodology

The uncertainty of an experimental system is comprised of three components: calibration errors, data acquisition errors, and data reduction errors (Ref. 7). Calibration and data acquisition errors will be considered in detail, but because data reduction errors are typically negligible (consisting mainly of computer round-off or truncation errors which, in this case, are of very small magnitudes), this contribution to the total uncertainty was not included. For each type of measurement taken (i.e., pressure, temperature, etc.), a list of elemental sources of error was compiled and estimates of each component error was made. See Tables I through III. Included in the tables are a description of the elemental sources of error which contribute to the calibration and data acquisition components of the total precision error. Since this is a pretest analysis, the estimated values for data acquisition errors were obtained from past test results and are assumed to include all of the sources listed in the tables.

Errors can be either random (precision) or fixed (bias). Reference 7 describes these errors in greater detail. For this analysis, it was assumed that calibration of the instrumentation immediately before testing eliminates all large, known biases, good, well-established test techniques eliminate sources of large, unknown bias error, and small, known and unknown bias errors are negligible. Therefore, all bias errors were assumed to be zero.

Since this is a pretest analysis, test data from a previous single rocket engine firing were used to provide representative values of the data acquisition errors for each measurement device.

The calibration errors of each instrument was determined by taking the square root of the sum of the squares (also known as root sum square, or RSS) of the elemental sources of calibration error. Traceability to the National Bureau of Standards was possible by obtaining calibration data (hysteresis and nonlinearity) from an independent calibration service.

The standard estimate of error (SEE) of the prior test raw data was obtained by using a linear curve fit. This accounted for time varying engine conditions by modeling the parameter as a function of time. The RSS value of the SEE and the other sources of data acquisition error result in a total data acquisition error value.

Knowing the calibration and data acquisition errors for each of the measured parameters, these errors are then propagated from the measured parameters to the calculated quantities. This is done by the expression

$$s_{x_j} = \sqrt{\sum_{k=1}^{m}\left(\frac{\partial x_j}{\partial x_k} s_{x_k}\right)^2} \qquad (8)$$

where m is the number of terms used to compute x_j (Ref. 7). Equation (8) requires the definition of influence coefficients which are the partial derivatives of the calculated parameters with respect to each variable (Ref. 7). Influence coefficients describe the effect of a unit change of one parameter with one set of units on the calculated parameter, with another set of units. These partial derivatives are multiplied by the corresponding precision errors and the RSS is computed to determine the final error for that parameter. Where partial derivatives were unattainable, perturbation techniques are described in Ref. 7 to calculate the influence coefficients.

Table IV lists the calculated parameters, the expression for the influence coefficients and values for each influence coefficient from a previous test.

Because the thermodynamic properties of the propellants upstream of the venturi were computed using GASP, the perturbation technique was required to determine the appropriate influence coefficients. The nominal values of line pressure and temperature were individually perturbed by ±1 percent and the ratio of the differences of each of the calculated quantities (line density, enthalpy, and entropy) to the differences of the perturbed quantity resulted in a value for the influence coefficients. GASP was again used to determine the density, temperature, and enthalpy at the venturi throat knowing the throat pressure and entropy. The same perturbation method was used to determine the influence coefficients for this case.

The degrees of freedom (ν) of a parameter indicates approximately how large the data sample size is for a given test and depends upon the type of curve fit used to characterize the data. The degrees of freedom of the measured and calculated parameters was computed using the Welch-Satterthwaite formula:

$$\nu_{x_j} = \frac{\left[\sum_{k=1}^{m}\left(\frac{\partial x_j}{\partial x_k} s_{x_k}\right)^2\right]^2}{\sum_{k=1}^{m}\left(\frac{s_{x_k}^4}{\nu_{x_k}}\right)} \qquad (9)$$

(Ref. 7) and made use of the influence coefficients and propagated SEE values mentioned above.

One method to determine measurement uncertainty using the propagated precision and bias errors and the degrees of freedom, is the additive technique (Ref. 7). It is expressed as

$$U_{99} = \pm\left(B + \frac{t_{95}}{\sqrt{n}} S\right) \qquad (10)$$

where B and S are the RSS bias and precision values of calibration and data acquisition errors, respectively. Because all bias errors were assumed to be zero for this pretest analysis, Eq. (10) becomes

$$U_{99} = \pm \frac{t_{95}}{\sqrt{n}} S \qquad (11)$$

Uncertainty Analysis

As mentioned previously, the uncertainty analysis described above was carried out using data from past tests for the data acquisition errors. Line-of-best-fit equations for the propellant line pressures, differential pressures, line temperatures, the site thrust, and test capsule ambient pressure were used to describe the time varying behavior during unsteady operation of the rocket engine. Actual data were used for hardware diameters and venturi discharge coefficients.

Calibration errors of six instruments were parametrically varied in the following manner. The first instrument calibration error was varied over its entire range. The second instrument calibration error was then incremented and the first was again cycled over its entire range of values. In this manner the second variable cycled through its range of values, at which time the third instrument calibration error was incremented. In this odometer-like fashion, all six variables were cycled trying all the combinations of calibration errors for all six instruments. Each instrument's calibration error was varied over a wide range of values (as shown in Table V) and the uncertainties for all the calculated quantities were computed. The ranges selected for each instrument's calibration precision error encompassed values typical for each type of instrument from prior tests. For example, if a thermocouple had a 0.04 R calibration error, the range from 0.01 to 0.10 R was selected for this study. The data acquisition errors were constant for each variation of calibration errors tried.

RESULTS AND DISCUSSIONS

Specific impulse is the prime performance parameter. Therefore, the uncertainty of specific impulse was used to indicate whether or not a given set of calibration uncertainties was acceptable. A goal of 1 percent uncertainty on specific impulse was chosen to represent a realistic limit of maximum allowable error due to the instrumentation system. Hence, the resulting plots (Figs. 2 to 5) display specific impulse uncertainty as a function of the six instruments whose calibration error was parametrically varied.

Figure 2 is a representative plot which resulted from the parametric uncertainty analysis. Vacuum specific impulse uncertainty as a function of oxidizer differential pressure calibration precision error with lines of constants oxygen line temperature calibration precision error are plotted. The four parameters which remain constant in this plot are the calibration precision errors of: oxidizer and fuel line pressure, fuel differential pressure, and fuel line temperature. As can be seen in Fig. 2, as the oxygen differential pressure and line temperature precision error increased, the uncertainty of I_{sp} increased at a nonlinear rate.

Within the parametric ranges investigated, the following generalized results were evident:

(1) The uncertainty of vacuum specific impulse always exceeded 1.0 percent for oxygen line pressure calibration precision error greater than or equal to 0.4 psia and for fuel line pressure calibration precision error greater than or equal to 3.0 psia. Values of I_{sp} uncertainty less than 1.0 percent were achieved, however, with lower values for these two parameters.

(2) Parameters which produced changes in the uncertainty value of vacuum specific impulse by much less than 1 percent included the calibration precision error of fuel line temperature.

(3) Changes in fuel differential pressure calibration precision error produced changes of approximately 1 percent in the uncertainty value of vacuum specific impulse.

(4) Greater than 1 percent changes to the uncertainty value of I_{sp} were caused by oxygen differential pressure and oxygen line temperature calibration precision error changes.

By simply crossplotting the data shown in Fig. 2, a second set of uncertainty plots was created by plotting oxygen line temperature calibration precision error versus oxygen differential pressure calibration precision error with lines of constant I_{sp} uncertainty. In Fig. 3, the I_{sp} uncertainty value of 1.0 percent is shown in this format. By isolating the 1 percent uncertainty line, a plot with five curves is used to produce a plot with one curve. In the cases where the lines did not cross the unity uncertainty line, linear extrapolation including only the last five data points was used to provide an estimate of the intersection point. Any point on the curve in Fig. 3 defines an instrument combination which results in a vacuum specific impulse uncertainty of 1.0 percent. In the region above the curve, the uncertainty is greater than 1.0 percent and in the region below the curve, the uncertainty is less than 1.0 percent. It can be seen that an oxidizer thermocouple with a high calibration error can be compensated for with the proper oxidizer differential pressure transducer.

By adding the complete set of fuel differential pressure calibration error data to this plot, a family of curves results (Fig. 4). Each of these curves has the property of defining a unity uncertainty boundary for different fuel differential pressure calibration precision error values.

Instead of varying the calibration precision error of the fuel differential pressure (resulting in Fig. 4), a family of fuel line temperature curves could be generated (Fig. 5). The "spread" between unity uncertainty lines for the fuel line temperature is not as great as that for the fuel differential pressure. This indicates a greater influence of the fuel differential pressure on I_{sp} uncertainty than the fuel line temperature.

By carefully selecting the measurement devices and placing them in the proper locations, this study shows that 1 percent specific impulse uncertainty is attainable. However, the cost of instrumentation to achieve this limit has not been addressed and is beyond the scope of this paper. Still, by putting measurement devices in parallel and/or series configurations to get redundant data, or to increase the number of collected data points, the value of specific impulse uncertainty can be lowered further. The JANNAF goal of 0.25 percent may be achievable, but the effort required to attain this limit may not be practical.

CONCLUDING REMARKS

An uncertainty analysis of the liquid rocket engine test set-up at NASA Lewis is described. Pretest uncertainty analyses were conducted by parametrically varying the calibration sources of error for each instrument in an attempt to determine calibration error limits on different instruments to assure a maximum uncertainty of 1.0 percent on vacuum specific impulse.

The I_{sp} uncertainty was found to increase at a nonlinear rate with the calibration precision error of all the measurement devices. Changes in oxygen delta pressure and line temperature calibration precision error affected the specific impulse uncertainty by more than 1.0 percent. Other parameters were seen to affect I_{sp} uncertainty by approximately 1.0 percent.

This parametric study quantifies how precise all the measurement instruments, taken as a group, must be to achieve a given uncertainty goal. An oxygen line pressure calibration precision error of 0.1 psia was acceptable, but a value of 0.4 psia was too large. A fuel line pressure calibration precision error of 1.0 psia was acceptable but a value of 3.0 psia led to unacceptable uncertainty values. By carefully selecting the measurement devices and placing them in the proper locations, this study shows that 1 percent specific impulse uncertainty is attainable.

APPENDIX A

Symbols

A area

B combined bias error

C_d venturi discharge coefficient

d diameter

dp static pressure difference between the propellant line and the venturi throat

F thrust

h enthalpy

I_{sp} specific impulse

K conversion factor, 50079.6 $\left[\frac{(ft/sec)^2}{Btu/lbm}\right]$

$\dot{m}$ mass flow rate

n number of points in test sample

p static pressure

S combined precision error

s component precision error

t_{95} student's "t"

U_{99} uncertainty encompassing 99 percent of data

V velocity

x variable

β propellant line contraction ratio

ν degrees of freedom

ρ density

Subscripts

exit nozzle exit plane

fu fuel

i oxidizer or fuel

j index

k index

line propellant line

ox oxidizer

site site

th venturi throat

TOT total (i.e., combined propellants)

vac vacuum

REFERENCES

1. Praharaj, S.C. and Palko, R.L.; "Measurements For Rocket Engine Performance Code Verification," Report RTR 157-01, REMTECH, Inc., Oct. 1986.

2. Abernethy, R.B.; Colbert, D.L.; and Powell, B.D.; "ICRPG Handbook for Estimating the Uncertainty in Measurements Made With Liquid Propellant Rocket Engine Systems," CPIA-180, Chemical Propulsion Information Agency, Laurel, MD, Apr. 1969.

3. Nagel, N.; "RL-10 Performance Parameter Uncertainty," Interoffice Correspondence, United Aircraft Corporation, Pratt & Whitney Aircraft, Dec. 27, 1968.

4. "Measurement Uncertainty for Fluid Flow in Closed Conduits," ANSI/ASME MFC-2M, 1983.

5. "Uncertainty of In-Flight Thrust Determination," SAE AIR-1678, 1985.

6. Abernethy, R.B. and Thompson, J.W., Jr; Uncertainty in Gas Turbine Measurements, Revised Edition, Instrument Society of America, 1980.

7. Abernethy, R.B. et. al.; Handbook, Uncertainty in Gas Turbine Measurements. AEDC-TR-73-5, Feb. 1973.

8. Pavli, A.J.; Kacynski, K.J.; and Smith, T.A.; "Experimental Thrust Performance of a High Area-Ratio Rocket Nozzle," proposed NASA Technical Paper, 1987.

9. Hendricks, R.C.; Baron A.K.; and Peller, I.C.; "GASP - A Computer Code for Calculating the Thermodynamic and Transport Properties for Ten Fluids: Parahydrogen, Helium, Neon, Methane, Nitrogen, Carbon Monoxide, Oxygen, Fluorine, Argon, and Carbon Dioxide," NASA TN D-7808, 1975.

TABLE I. - SOURCES OF ELEMENTAL ERROR IN PRESSURE MEASUREMENTS

Calibration errors due to ...	Comments
Zero reading error	Instruments are zeroed before data-taking
Standards lab calibration of the transducer calibration, including NBS traceability	Errors of standards lab's instruments
Changes in transducer calibration pressure	Not applicable
Transducer hysteresis	Independent calibration
Transducer nonlinearity	Independent calibration
Data acquisition errors due to ...	**Comments**
Transducer temperature difference at zero balance	Negligible because lines were at room temperature
Transducer temperature difference at data-taking	Negligible because lines were at room temperature
Determination of reference pressure	Independent calibration
Changes in temperature on the transducer	Negligible because lines were at room temperature
Effect of vibration on the transducer	Negligible because propellant lines are damped
Effect of changes in line pressure	Line pressure changes were negligible during testing
Ability to determine a representative value over a specified time interval as data varies	Data averaging reduces error to negligible magnitude. Each point consists of five samples taken at 1 sample/1 ms and and line-of-best-fit used
Signal conditioning, electrical calibrations, and digital system	Based on past data from other test facilities at NASA Lewis

TABLE II. - SOURCES OF ELEMENTAL ERROR IN TEMPERATURE MEASUREMENTS

Calibration errors due to ...	Comments
Zero reading error	Instruments are numerically zeroed before data-taking
Manufacturer's specification of wire calibration	Manufacturer's specifications
Reference temperature level determination	Manufacturer's specifications
Data acquisition errors due to ...	**Comments**
T/C temperature difference at zero balance	Negligible because lines were at room temperature
T/C temperature difference at data-taking	Negligible because lines were at room temperature
Fabrication of T/C	As per standards
Effect of vibration on the transducer	Negligible because propellant lines are damped
Effect of changes in line pressure	Line pressure changes were negligible during testing
Reference temperature stability	±0.25 percent
T/C design due to radiation, friction, etc., when measuring gas temperatures	Good design practice reduces this to negligible magnitude
Heat conduction	All parts at uniform temperature
Temperature gradients along non-homogeneous T/C wire	All parts at uniform temperature
Ability to determine a representative value over a specified time interval as data varies	Data averaging reduces error to negligible magnitude. Each point consists of five samples taken at 1 sample/1 ms and line-of-best-fit used
Signal conditioning, electrical calibrations, and digital system	Based on past data from other test facilities at NASA Lewis

TABLE III. - SOURCES OF ELEMENTAL ERROR OF THRUST MEASUREMENT

Calibration errors due to ...	Comments
Standards lab calibration of the transducer calibration, including NBS traceability	Errors of standards lab's instruments
Thrust stand hysteresis and non-linearity	±0.5 percent as per manufacturer's specifications
Shift in load cell calibration caused by attachment of adaptors/ flexures	Physical set-up reduces these to negligible magnitude
Data acquisition errors due to ...	**Comments**
Zero reading error	Instruments are numerically zeroed before data-taking
Effect of vibration on the load cell	Negligible
Effect of vibration on the thrust stand	Negligible
Misalignment between the engine force vector and the force vector measured by the data load cell train	Triad arrangement accounts for misalignment
Measurement of forces on an axis different from the engine center-line	Triad arrangement accounts for misalignment
Pressurization on the load cell	Corrected by aneroid calibration
Effect of changes in cell pressure test cell wall	Cell wall is not ground for load cell
Effect of changes in line pressure on tare forces exerted on thrust measurement system by propellant lines, etc., routed to engine	Physical set-up reduces these to negligible magnitude
Effect of changes in temperature on the load cell	Temperature changes were negligible during calibration and testing
Thermal growth of the thrust stand	Negligible
Secondary airflow effect on the load cell	Negligible during steady-state operation
Ability to determine a representative value over a specified time interval as data varies	Data averaging reduces error to negligible magnitude. Each point consists of five samples taken at 1 sample/ 1 ms and line-of-best-fit used
Signal conditioning, electrical calibrations, and digital system	Based on past data from other test test facilities at NASA Lewis

TABLE IV. - INFLUENCE COEFFICIENT EXPRESSIONS AND TYPICAL VALUES

Calculated parameter	Influence coefficients	Ox/Fu Typical value
p_{th} Pressure at the venturi throat	$\frac{\partial p_{th}}{\partial p_{line}} = 1$	1/1
	$\frac{\partial p_{th}}{\partial dp} = 1$	-1/-1
β Line contraction ratio	$\frac{\partial \beta}{\partial d_{th}} = \frac{1}{d_{line}}$	0.62/0.62
	$\frac{\partial \beta}{\partial d_{line}} = -\frac{d_{th}}{(d_{line})^2}$	-.16/-.17
V_{th} Velocity at the venturi throat	$\frac{\partial V_{th}}{\partial h_{line}} = \frac{\sqrt{K}}{2}\left\{(h_{line} - h_{th})\left[1 - \left(\frac{\rho_{th}}{\rho_{line}}\right)^2 \beta^4\right]\right\}^{-1/2}$	103/19
	$\frac{\partial V_{th}}{\partial h_{th}} = -\frac{\partial V_{th}}{\partial h_{line}}$	-103/-19
	$\frac{\partial V_{th}}{\partial \rho_{line}} = -\frac{(\rho_{th})^2}{(\rho_{line})^3} \frac{V_{th}\beta^4}{\left[1 - \left(\frac{\rho_{th}}{\rho_{line}}\right)^2 \beta^4\right]}$	.23/29
	$\frac{\partial V_{th}}{\partial \rho_{th}} = -\frac{\rho_{th}}{(\rho_{line})^2} \frac{V_{th}\beta^4}{\left[1 - \left(\frac{\rho_{th}}{\rho_{line}}\right)^2 \beta^4\right]}$	.24/31
	$\frac{\partial V_{th}}{\partial \beta} = \left(\frac{\rho_{th}}{\rho_{line}}\right)^2 \frac{2V_{th}\beta^3}{\left[1 - \left(\frac{\rho_{th}}{\rho_{line}}\right)^2 \beta^4\right]}$	7.4/48

TABLE IV. - Concluded.

Calculated parameter	Influence coefficients	Ox/Fu Typical value
$\dot{m}$ Propellant mass flow rate	$\frac{\partial \dot{m}}{\partial (C_d A_{th})} = \rho_{th} V_{th}$	6.5/1.9
	$\frac{\partial \dot{m}}{\partial \rho_{th}} = C_d A_{th} V_{th}$	.21/1.4
	$\frac{\partial \dot{m}}{\partial V_{th}} = C_d A_{th} \rho_{th}$	.003/.0002
$\dot{m}_{TOT}$ Total mass flow rate	$\frac{\partial \dot{m}_{TOT}}{\partial \dot{m}_{ox}} = 1$	1
	$\frac{\partial \dot{m}_{TOT}}{\partial \dot{m}_{fu}} = 1$	1
F_{vac} Vacuum thrust	$\frac{\partial F_{vac}}{\partial F_{site}} = 1$	1
	$\frac{\partial F_{vac}}{\partial p_{amb}} = A_{exit}$	815
	$\frac{\partial F_{vac}}{\partial A_{exit}} = p_{amb}$	.037
I_{sp} Specific impulse	$\frac{\partial I_{sp}}{\partial F_{vac}} = \frac{1}{\dot{m}_{TOT}}$	0.89
	$\frac{\partial I_{sp}}{\partial \dot{m}_{TOT}} = -\frac{F_{vac}}{(\dot{m}_{TOT})^2}$	-427

TABLE V. - RANGES OVER WHICH EACH INSTRUMENT CALIBRATION PRECISION ERROR WAS VARIED

Parameter, units	Values		
	Minimum	Maximum	Increment
Ox line pressure, psia	0.1	2.8	0.3
Fu line pressure, psia	1.0	9.0	2.0
Ox differential pressure, psid	.01	.28	.03
Fu differential pressure, psid	.1	.9	.2
Ox line temperature, R	.01	.10	.01
Fu line temperature, R	.01	.09	.02

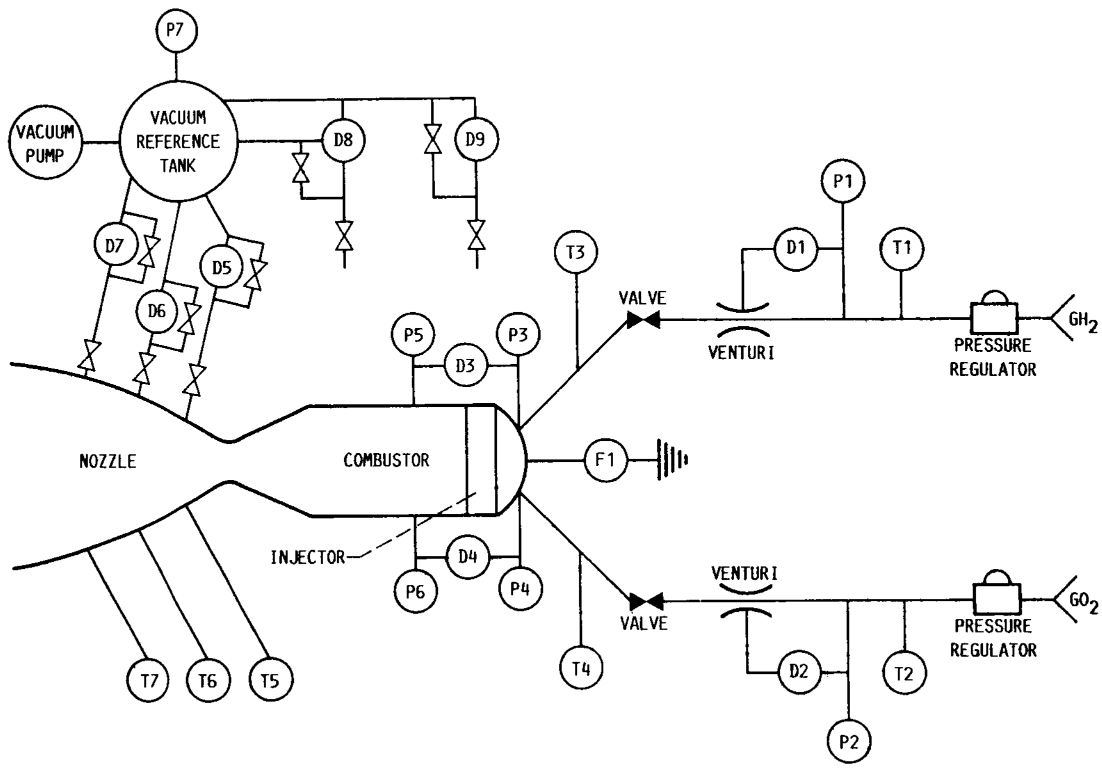

D1	FUEL VENTURI ΔP	D9	ALTITUDE ΔP	P7	VACUUM REFERENCE PRESSURE
D2	OXYGEN VENTURI ΔP	F1	THRUST	T1	FUEL SUPPLY TEMPERATURE
D3	FUEL INJECTION ΔP	P1	FUEL SUPPLY PRESSURE	T2	OXYGEN SUPPLY TEMPERATURE
D4	OXYGEN INJECTION ΔP	P2	OXYGEN SUPPLY PRESSURE	T3	FUEL INJECTION TEMPERATURE
D5	NOZZLE WALL ΔP	P3	FUEL INJECTION PRESSURE	T4	OXYGEN INJECTION TEMPERATURE
D6	NOZZLE WALL ΔP	P4	OXYGEN INJECTION PRESSURE	T5	NOZZLE WALL TEMPERATURE
D7	NOZZLE WALL ΔP	P5	CHAMBER PRESSURE	T6	NOZZLE WALL TEMPERATURE
D8	ALTITUDE ΔP	P6	CHAMBER PRESSURE	T7	NOZZLE WALL TEMPERATURE

FIGURE 1. - ROCKET ENGINE TEST SET-UP AND INSTRUMENTATION SCHEMATIC.

CONSTANTS

PARAMETER	VALVE
Ox LINE PRESS	0.1 PSIA
Fu LINE PRESS	1.0 PSIA
Fu DIFF. PRESS	0.9 PSID
Fu LINE TEMPERATURE	.09 R

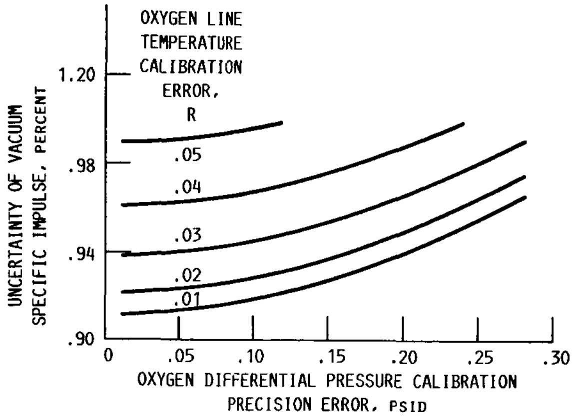

FIGURE 2. - SPECIFIC IMPULSE UNCERTAINTY VERSUS OXYGEN PRESSURE DIFFERENTIAL CALIBRATION ERROR FOR DIFFERENT OXYGEN LINE TEMPERATURE CALIBRATION ERRORS.

FUEL PRESSURE DIFFERENTIAL CALIBRATION PRECISION ERROR = 0.9 PSID
CAL PRECISION ERROR OF Ox LINE PRESS = 0.1 PSIA
CAL PRECISION ERROR OF Fu LINE PRESS = 1.0 PSIA

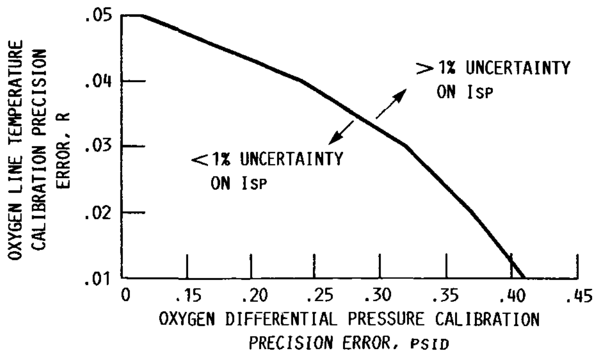

FIGURE 3. - UNCERTAINTY OF VACUUM SPECIFIC IMPULSE = 1 PERCENT FOR HYDROGEN LINE TEMPERATURE CALIBRATION PRECISION ERROR = .09 R.

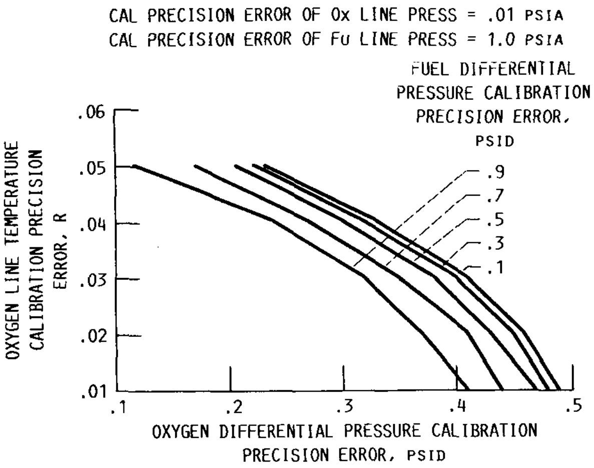

FIGURE 4.- UNCERTAINTY OF VACUUM SPECIFIC IMPULSE = 1 PERCENT FAMILY OF CURVES FOR HYDROGEN LINE TEMPERATURE CALIBRATION PRECISION ERROR = .09 R.

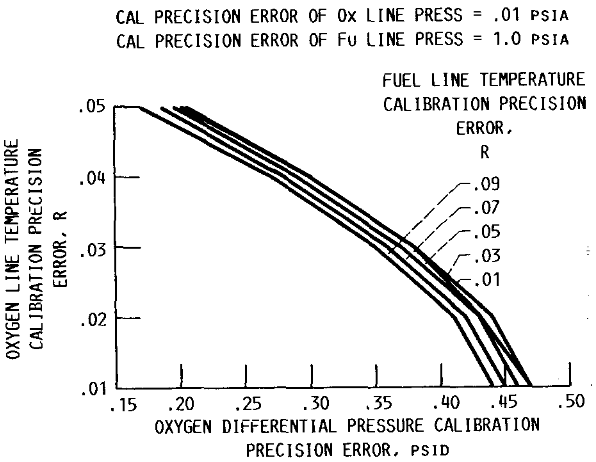

FIGURE 5. - UNCERTAINTY OF VACUUM SPECIFIC IMPULSE = 1 PERCENT FAMILY OF CURVES FOR HYDROGEN DELTA PRESSURE CALIBRATION PRECISION ERROR = 0.7 PSID.

1. Report No.	2. Government Accession No.	3. Recipient's Catalog No.
NASA TM-89819		
4. Title and Subtitle Pretest Uncertainty Analysis for Chemical Rocket Engine Tests		5. Report Date
		6. Performing Organization Code 506-42-21
7. Author(s) Kenneth J. Davidian		8. Performing Organization Report No. E-3465
		10. Work Unit No.
9. Performing Organization Name and Address National Aeronautics and Space Administration Lewis Research Center Cleveland, Ohio 44135		11. Contract or Grant No.
		13. Type of Report and Period Covered Technical Memorandum
12. Sponsoring Agency Name and Address National Aeronautics and Space Administration Washington, D.C. 20546		14. Sponsoring Agency Code

15. Supplementary Notes

Prepared for the 33rd International Instrumentation Symposium, sponsored by the Instrument Society of America, Las Vegas, Nevada, May 3-8, 1987.

16. Abstract

A parametric pretest uncertainty analysis has been performed for a chemical rocket engine test at a unique 1000:1 area ratio altitude test facility. Results from the parametric study provide the error limits required in order to maintain a maximum uncertainty of 1 percent on specific impulse. Equations used in the uncertainty analysis are presented.

17. Key Words (Suggested by Author(s))	18. Distribution Statement
Uncertainty analysis; Measurements; Error; Rocket engine	Unclassified - unlimited STAR Category 35

19. Security Classif. (of this report)	20. Security Classif. (of this page)	21. No. of pages	22. Price*
Unclassified	Unclassified	15	A02

*For sale by the National Technical Information Service, Springfield, Virginia 22161